High Efficiency Multijunction Tandem Solar Cells with Embedded Short-Period Superlattices

Argyrios C. Varonides[1,*]

[1]*University of Scranton, 800 Linden Street, Scranton Pennsylvania 18510, USA*
** Corresponding author. Tel: +1(570)941-6290, Fax: +1(570) 941-4015, E-mail: varonides@scranton.edu*

Abstract: We propose a 1cm^2 tandem solar cell with different lattice-matched materials based on a 2eV/1.42eV/0.66eV energy gap sequence. The top unit is a p-n-n AlAs/GaAs cell, connected in series with a bottom cell which is a bulk GaAs/Ge p-n-n cell; a narrow GaAs/Ge superlattice region embedded in the middle region. Transition of carriers between the two units is possible via a tunnel junction connecting the two units. More specifically, the upper cell is a 20 μm bulk p-n-n cell tuned to the visible range of the solar spectrum, producing short circuit currents near 30mA/cm^2, and open-circuit voltage (OC) of 1.04V; the bottom cell is an 80 μm bulk p-n-n GaAs/Ge with an embedded GaAs/Ge superlattice tuned at 1eV. The bottom cell produces short circuit current density at18.5 mA/cm^2 in the bulk; however a 20-period GaAs/Ge embedded short superlattice provides an additional 10 mA/cm^2 thermionic current density, so that total bottom current reach 28.5mA/cm^2, in close matching (5%) with the top currents, and an OC voltage of 0.968V. The tandem cell's basic parameters are (a) average fill factor of (FF) 85% (b) short circuit current 28.5 mA/cm^2 and (c) OC voltage 2.008V (due to the series connection); for 100mW/cm^2 standard solar radiation, collection efficiency of such a device is depicted in excess of 47% under one sun. Such small area cells are useful for CPV for their minimized size and material requirements.

Keywords: *Solar cells, Superlattices, Tuned quantum wells, High efficiency photovoltaics*

Nomenclature

J_{TH} *thermionic current density …....mA/cm^2*
J_{sc} *short-circuit current.…..…..…....mA/cm^2*
V_{oc} *open-circuit voltage.……..…..…..Volts*
L_w *quantum well width.…..……..…..…nm*
n_{ph} *photo-excited carriers ……..…..…..…...cm^{-3}*
g_o, *g(E) density of states.……..…..…...eV^{-1}cm^{-2}*
g_o, *g(E) density of states.…..…..…...eV^{-1}cm^{-2}*

1. Introduction

The field of high efficiency photovoltaics (HEPV) is maturing steadily; already the threshold of 40% efficiency has been reached and exceeded to 42.2 % [1, 2, 3, 4, 5, 6]. It is common place in the PV community that the 50% limit for crystalline solar cells will be within reach in the next five years. The common denominator of high efficiency cells is the idea of two to three different band gaps that absorb in different wavelengths, preferably in a successive fashion along with the visible and the infrared parts of the solar spectrum. A typical cell of such geometry contains three major layers of lattice-matched or suitably metamorphic semiconductor layers joined (in series) by means of tunnel junctions. The latter are needed to ensure current matching. The obvious advantage of such structures is the series connection of two p-n junctions essentially, with increased overall open circuit voltage (due to the series connection). In this communication we are proposing an ostensibly high efficiency structure based on the series connection idea, as mentioned above, but with a different design, especially in the area of long wavelength absorption. The latter is a process that can be realized by means of two dimensional geometry selections (or one dimensional option as well). The device is described in brief as follows: a top p-n or p-i-n bulk GaAs/AlAs/Alloy cell is proposed for short wavelength absorption (mainly visible). The unit is then grown on top of a tunnel junction (guaranteeing the series connection) and the bottom cell follows with a similar topography, namely, a p-i-n cell matched with the layers above it. The intrinsic region of this cell is replaced by a GaAs/Ge superlattice with reduced tunneling. The latter

selection is adopted for two reasons (a) Ge is lattice-matched with GaAs and (b) we want to ensure thermal current generation from the mid- (intrinsic/low-doped) to the n-region of the device, as shown in Figure 1 below:

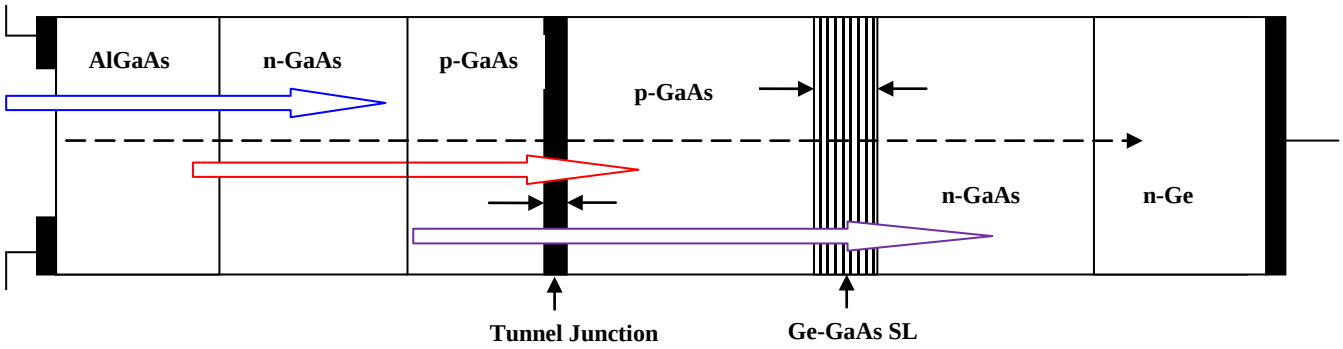

Fig. 1 Proposed tandem (1cm^2) p-n-n$^+$/p-n (Superlattice (SL))-n$^+$ multijunction solar cell, for high efficiency. Two cells in series through a tunnel junction. Maximum current density depicted at 28.5mA/cm^2; Open-circuit voltage values 1.04 and 0.968V respectively. Total V_{oc} = 2.008V, J_{sc} = 30mA/cm^2.

The structure promotes the series connection of two cells, with current matching. As seen from the figure above, the goal is to produce a composite cell where both short and long wavelengths are absorbed simultaneously; in this context, this can be succeeded via the two layers shown. Visible and near infrared absorption is guaranteed by the two cells respectively, while the MQW geometry is tuned to longer wavelengths via pre-selected eigen-state resonance. Therefore, analysis and simulation of the device will have to include both regions as depicted through (a) the top and (b) bottom cells and (c) through the tunnel junction (TJ). The latter is basically selected to be a double barrier heterostructure of p^{++} and n^{++} highly doped GaAs layers (TJ modeling for this purpose will be reported elsewhere). Fundamentally, photoelectrons induced from the top, tunnel through the mid-junction to join carriers from the lower cell. Ultimately, due to the series connection, matching will dictate the final current, in other words, the lowest current will keep the connection at the ON state. On the other hand, the series connection is expected to provide enhanced voltage (ideally the sum of the two OC voltages as they come from the two sub-cells). It is imperative therefore to model all regions for optimum current and voltage generation. In the following sections, modeling and simulations for two of the three mentioned regions is provided as a tool for optimization in design.

2. Top Cell for the visible solar spectrum

It is desirable to obtain a top layer suitable for visible spectrum absorption. Graded AlGaAs layers of variable aluminum fractional content is proposed according to the following table:

Table 1: Bandgap and wavelength at different Aluminum percentage content for AlGaAs

Al content (%)	Band-gap (eV)	Wavelength λ(μm)
0.98 (AlAs)	2.16	0.574
0.90	2.11	0.582
0.80	2.07	0.592
0.70	2.05	0.602
0.60	2.02	0.612
0.50	1.998	0.620

As seen from the table above, a feasible succession of lattice-matched AlAs-AlGaAs graded layer ensures visible spectrum absorption. Modeling of a 0.5 to 1.0μm p-AlAs/AlGaAs layer on top of an n-n^+ GaAs arrangement (upper part of Figure 1) leads to short circuit current at 30.50 mA/cm^2, and open-circuit (*OC*) voltage at 1.04V, with max power 28.30 mW [temperature 300 ^oK; one-sun exposure and power input of 100mW/cm^2; 10% internal reflection]. Figure 2 shows the J-V characteristics of the top cell, where both current-voltage and power-current curves are depicted. This is a high current solar cell and can stand alone. Note also that with an 88 to 90% fill factor (*FF*), this is a 27.9 % cell. Note also that a second junction could be used as the bottom cell, with exactly the same characteristics; in such a case, one (provided the tunnel junction can sustain 30mA/area) may end up with a double junction cell with 2V and 30mA/unit area, which would lead to a double-junction cell (area 1square centimeter) with collection efficiency with collection efficiency n(%) = (2x30mA/cm^2) x (FF)/(100mW/cm^2). For a collective fill factor near 80%, this leads to 48% collection efficiencies. Figure-2 below depicts a simulated J-V characteristic (extrapolation to the horizontal axis leads to 1.04V):

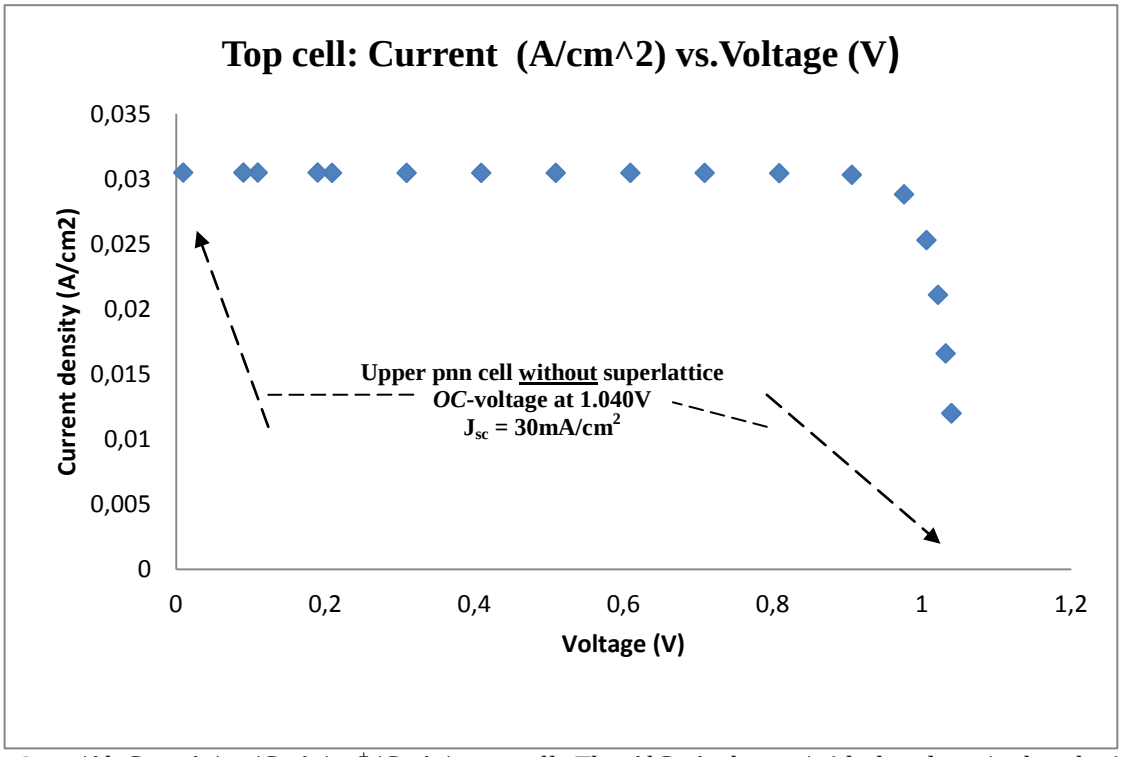

Fig.2. p ($Al_xGa_{1-x}As$)-n(GaAs)-n^+(GaAs) top cell. The AlGaAs layer (wide band gap) absorbs in the visible (see Table 1). Max current and OC-voltage extrapolated at 30.5mA/cm^2 and 1.04V respectively.

3. Bottom Cell

Out of several options for a double junction cell, we select a p-n-n *1.82eV/1.42eV/0.66eV* cell in order to demonstrate two points (a) to include long wavelength absorption and (b) to introduce the idea of tuning layers in the mid-regions to desired wavelengths. In this paper we are proposing a quantum well structure embedded in the mid-region of the bottom cell and tuned to 1eV solar photons. Regarding the 0.66 eV material (for long wavelengths: 1.24/0.66 = 1.878 μm) include in the bottom cell design, simulations lead to short circuit current density at J_{sc} = 18.50 mA/cm^2 and *OC*-voltage V_{oc} = 0.968V. Simulation and modeling of the bottom unit is basically in a structure depicted by lower portion of Figure-1, *without* the mqw region. The mqw region is a 20-period GaAs/Ge superlattice (no tunneling) with thin Ge-quantum

wells tuned at 1eV or with a 19.6 nm width. Potential barriers are selected at 100nm (in order to minimize tunneling). The total thickness of the reduced dimensionality superlattice is 20 x (200+19.6) = 4,392 nm = 4.392 μm; the latter is just 5.3% of the total lower cell, which is essentially a pnn GaAs/Ge solar cell with its J-V graph shown by figure-3:

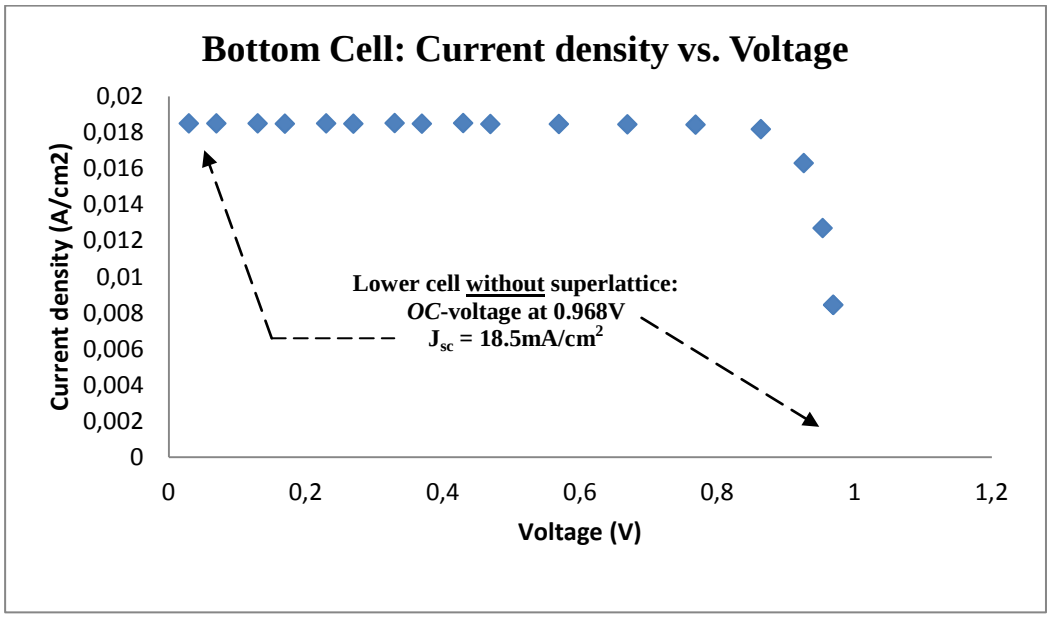

Fig. 3: Bottom cell J-V characteristics: a bulk pnn GaAs/Ge cell with 0.968V and 18.5mA/cm^2 (OC and SC) parameters respectively.

By proposing a superlattice in the mid region of the lower cell (in future designs this could be proposed for both cells as well!) we actually introduce a second channel of carrier current per unit area, such that the current in the lower part of the device might go increase as well. In the next section, we develop a formalism of thermionic current escape that contributes to the main bulk current of the bulk device as depicted in Figure-4 below:

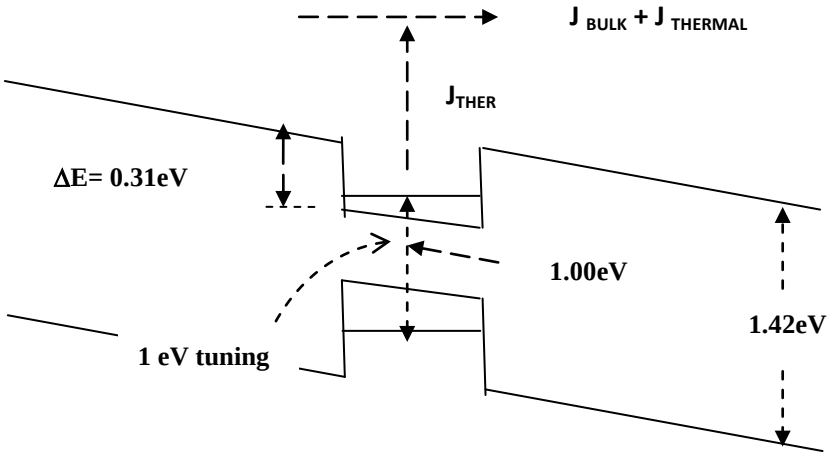

Fig. 4: Fine tuning at specific wavelengths can be achieved through quantum size effects in the traps of the intrinsic region. Electrons' thermionic conduction, from 20nm quantum wells, is schematically shown at the conduction band. Note the Fermi and intrinsic Fermi levels, and the addition of the two current components: bulk and thermal current components respectively.

Final current from the quantum traps adds constructively to the bulk current generated by the GaAs/Ge cell (18 mA/unit area, see Figure-3 above). Due to current matching, overall *SC*-current output is going to be based on the lowest current off the two cells. Thus, thermal escape generation becomes essential: simultaneous high current and voltage generation may lead to higher "ground" collection efficiency (one sun conditions). In the next section, modeling is geared towards thermionic current generation and current matching near $30mA/cm^2$.

4. Modeling of Thermionic current

As mentioned above and discussed elsewhere, photo-excitation forces excess carriers in quantum wells and an increase of total carrier population near 10^{12} cm^{-2}, per well [6]. Trapped photocarriers recombine and thermionically escape from the quantum traps. With recombination losses includes [8,9] and given that there is a non-zero probability for thermal escape, we model escaping carriers as thermionic currents over ΔE_C barriers. Once this is established, we consider the two current components as two current sources (in the bottom cell always), and we are adding these two components to find the total lower-cell current. In all probability, this result is not necessarily expected to match the top component, however, by imposing required conditions, selective doping and superlattice geometry; we expect total lower current to reach (as close as possible) the top one.

In the following, we briefly discuss this process. Thermionic emission from wells of depth ΔE_C leads to current density values of the type [8]:

$$j = q\int dxdEg(E)\,f(E)v(E)\delta n(x) \qquad (1)$$

Where q is the electronic charge, g(E) is the density of states (DOS) of the quantum trap (here quantum wells or quantum dots etc), f(E) is the Fermi level position in the gap of the semiconductor layer, v(E) is the "velocity" of the carriers at energy E and where δn(x) is the net carrier population in the traps of length/width L_W and after recombination. For an average excess carrier density $<\delta(x)> = \delta N = 10^{12}cm^{-2}$ per well, the above integral simplifies as follows:

$$j = q(\delta N)(L_W)g_o\int dEf(E)v(E) \qquad (2)$$

Thermionic currents can be calculated from the latter expression, where DOS represents the quantum system involved. In the present case we adopt quantum wells (faster and less cumbersome compared to quantum dots fabrication), where DOS is a constant function: (2-d DOS of quantum wells, $eV^{-1}cm^{-2}$). Based on the above and on the fact that the Fermi level is near (and above) 3(kT)'s below the conduction band of the low gap layer (E_C - E_F) (Fermi-Dirac approaches the Maxwell-Boltzmann distribution), the current relation yields the following explicit expression (by replacing for g(E) with g_o and relating the speed of the carriers with energy barrier ΔE_C of the heterojunction discontinuity):

$$j = q\times n_{ph}\times g_o\times L_W\times\sqrt{\frac{2}{m^*}}\times\int_E^\infty dE\sqrt{E-E_1}\times\exp(-\frac{E_1-E_F}{kT}) \qquad (3)$$

Where the difference $E-E_F$ is the activation energy relative to the Fermi level, E_1 is the lowest eigen-energy in the germanium quantum wells (near 10meV from the bottom of the wells, for

~20 nm width (L)). Note also that the excess carrier per unit area available per well is n_{ph}, and m* is the effective mass in germanium layers. Taking the lowest limit to be the ground eigen-state, the last expression leads to the following result:

$$j = q \times n_{ph} \times L_W \left(\frac{\sqrt{2\pi m^* k^3}}{\pi \hbar^2} \right) \times T^{3/2} \times \exp(-\frac{E_1 - E_F}{kT}) \quad (4)$$

Note from the above the dependence of the current on the activation energy through the exponential. For undoped germanium layers, activation energy values are the sum of eigen-energy value plus the $E_C - E_F$. The latter (for germanium) can be quickly computed [ ]:

$$\Delta E_{CF} = E_C - E_F = kT \ln(\frac{N_C^{Ge}}{n_i}) = 0.338eV \quad (5)$$

Where the factors in the fraction above are (a) the conduction band density and (b) the intrinsic concentration for Ge, and the 0.33 eV is essentially the intrinsic Fermi level. For such a result, our derived formula provides negligible thermal current (fraction of μA). For moderate doping levels near $10^{16}cm^{-3}$, we compute thermal currents 0.0429 mA/cm^2, which, for desired $10mA/cm^2$, would require a long superlattice (large number of periods, about 240). On the other hand, selecting doping levels near 10^{18} cm^{-3}, however, leads to current density near $0.4mA/cm^2$/well, which translates into 25 superlattice periods in all. Based on this, we propose an n-Ge/GaAs multi-junction layer in the middle region of the pnn GaAs/GaAs/Ge bulk lower cell, where total current will essentially reach the top-cell current and hence current matching will be succeeded within ~5% (note: top cell current $30mA/cm^2$, bottom cell currents: $18.5mA/cm^2$ plus $10mA/cm^2$ = $28.5mA/cm^2$). Based on this current matching and on the computed data (see short circuit currents, Figures 2 and 3), we estimate the following for the composite cell of Fig.-1: short circuit current of $28.5mA/cm^2$, and open circuit voltage $V_{oc1} + V_{oc2} = 1.04V + 0.968V = 2.008V$. This means that the composite cell (as long as the tunnel junction sustains normal operation) is expected to provide two volts at *OC* conditions and at least $28mA/cm^2$ at *SC* conditions. Both units of the tandem structure have fill factor values of 85 and 85.5 % respectively, as it can be found from the open-circuit voltages of each [12].Under one sun (AM 1.5), such a one-square centimeter tandem PV-device exhibits collection efficiency of [0.85x28.5x2]/100 = 48.45%. Obvious advantages in such a design are (a) minimal material usage (small area, and narrow superlattice layers; the latter suitable for growth technique selection (chemical vapor deposition or molecular epitaxy) (b) simultaneous short and long wavelength absorption (c) short-period tuned superlattice (d) high carrier mobility due to GaAs/Alloy major components (in contrast to mismatched cells with low mobility) (e) extension of design to include more than one superlattice tuned at desired wavelengths.

5. Conclusion

High efficiency solar cells are becoming a reality while collection efficiency levels near 40% have been achieved. It has been realized in recent years that more than one layer may lead to higher photon absorption due to varying energy band gaps involved. Indeed, this is the case for hetero-junction cells that include two or more materials in one unit; however, recently proposed tandems do not utilize superlattice components [5, 8]. In this paper we explore efficiency enhancement via (matched) current and voltage increase, with a 1eV-tuned superlattice embedded in one of the cells. Thus, a multijunction cell is proposed, with visible

and IR wavelength absorption capabilities. The proposed structured is a $1cm^2$ cell and is composed of two sub-cells: the bottom unit is a 20-period GaAs-Ge superlattice embedded in a pnn GaAs-Ge bulk solar cell. On top of this cell an AlAs-AlGaAs-GaAs cell is proposed, suitable for short wavelengths. The two units are connected in series via a standard tunnel junction, modeling of which is not discussed in this paper. Assuming ideality factors near one, modeling and simulation of the two devices shows a total voltage near 2 Volts and minimum current density 28.5 mA/cm^2. Collection efficiency is expected to exceed the 42% current threshold (one sun conditions). The cell structures involved, could individually perform well on their own at different wavelengths and with appreciable efficiencies respectively. Our proposed structure involves tuning of the lower device at desired photon energy input (1 eV). Under the same token, optimum tuning can be pre-arranged via specific superlattice geometry selections, while more than one superlattice in tandems seems to open the way for higher efficiencies. To probe further, two part-tandem cells, with a tuned superlattice in each region, should lead to collection efficiency in excess of 45% in the immediate future.

References

[1] M Yamaguchi et al, Super high-efficiency multijunction and concentrator solar cells, Solar Energy Materials & Solar Cells 90 (2006) 3068–3077

[2] AC Varonides, High Efficiency Lattice-Matched Multijunction Solar Cells via Tuned GaAs/Ge Quantum Wells25th European PVSEC, 2010

[3] M Yamaguchi et al, Novel materials for high-efficiency III–V multi-junction solarcells, Solar Energy 82, 173 (2008).

[4] R. King, et al, High Concentration PV Using III-V Solar Cells, 20th European PVSEC, 2005.

[5] Richard R. King, Daniel C. Law, Kenneth M. Edmondson, ChristopherM. Fetzer, Geoffrey S. Kinsey, Hojun Yoon, Dimitri D. Krut, James H. Ermer, Raed A. Sherif, and Nasser H. Karam, Advances in High-Efficiency III-V Multijunction Solar Cells, Hindawi Publishing Corporation, Advances in OptoElectronics, Volume 2007, Article ID 29523

[6] R Jones, J Ermer, P Pien, O Al Taher, R King, Spectrolab Progress in Multi-Junction Cell Performance and Cost, April 28-29, Toledo, Spain

[7] R.S. Miller, T.I. Kamins, Device Electronics for Integrated Circuits, J Wiley & Sons, 2nd Ed, 1986, pp 16-25

[8] C Algora, 2nd CPV Summit, April 28-29, Toledo, Spain.

[9] JF Geisz, S Kurz, MW Wanlass, JS Ward, A Duda, DJ Friedman, JM Olson, WE McMahon, TE Moriarty, and JT Kiehl, 40.8% efficient inverted triple-junction solar cell with two independently metamorphic junctions, Applied Phys. Letters 91, 023502 (2007).

[10] AC Varonides and RA Spalletta, Hopping currents in the intrinsic region of III-N-V quantum well structures in the tight binding approximation, Physica Stat. Sol. 5, No. 2 441 (2008)

[11] AC Varonides, Tunneling vs. Thermionic Currents in Multi-Quantum Well Photovoltaic, Structures, Physics E 14, 142 (2002)

[12] E. Lorenzo, Solar Electricity, Engineering of Photovoltaic Systems, Protomora General de Estudios, SA, 1994, Sevilla, Spain, p. 77